

# General Relativistic Stars : Polytropic Equations of State

Ulf S. Nilsson

*Department of Applied Mathematics  
University of Waterloo  
Waterloo, Ontario  
Canada, N2L 3G1*

and

*Department of Physics  
Stockholm University  
Box 6730  
S-113 95 Stockholm  
Sweden*

E-mail: unilsson@math.uwaterloo.ca

and

Claes Uggla

*Department of Physics  
University of Karlstad  
S-651 88 Karlstad  
Sweden*

E-mail: uggla@physto.se

In this paper, the gravitational field equations for static spherically symmetric perfect fluid models with a polytropic equation of state,  $p = k\rho^{1+1/n}$ , are recast into two complementary 3-dimensional *regular* systems of ordinary differential equations on compact state spaces. The systems are analyzed numerically and qualitatively, using the theory of dynamical systems. Certain key solutions are shown to form building blocks which, to a large extent, determine the remaining solution structure. In one formulation, there exists a monotone function that forces the general relativistic solutions towards a part of the boundary of the state space that corresponds to the low pressure limit. The solutions on this boundary describe Newtonian models and thus the relationship to the Newtonian solution space is clearly displayed. It is numerically demonstrated that general relativistic models have finite radii when the polytropic index  $n$  satisfies  $0 \leq n \lesssim 3.339$  and infinite radii when  $n \geq 5$ . When  $3.339 \lesssim n < 5$ , there exists a 1-parameter set of models with finite radii and a finite number, depending on  $n$ , with infinite radii.

*Key Words:* static spherical symmetry; stellar models; polytropic stars

## 1. INTRODUCTION

This paper is the second in a series dealing with general relativistic star models. Here we consider static spherically symmetric models. The line element for these models can be written as

$$ds^2 = -e^{2\phi(\lambda)} dt^2 + r(\lambda)^2 \left[ \tilde{N}(\lambda)^2 d\lambda^2 + d\Omega^2 \right] , \quad (1)$$

with

$$d\Omega^2 = d\theta^2 + \sin^2 \theta d\varphi^2 , \quad (2)$$

where  $\phi(\lambda)$  is the gravitational potential,  $r(\lambda)$  is the usual Schwarzschild radial parameter, and  $\tilde{N}(\lambda)$  a dimensionless (under scale-transformations) freely specifiable function. The choice  $\tilde{N} = 1$  corresponds to isotropic coordinates and the function  $\tilde{N}$  can hence be viewed as a relative gauge function with respect to the isotropic gauge. The coordinate  $\lambda$  is a spatial radial variable, defined by the choice of  $\tilde{N}$ .

The matter content of the star is assumed to be a perfect fluid, described by the energy-momentum tensor

$$T_{ab} = \rho u_a u_b + p (g_{ab} + u_a u_b) , \quad (3)$$

where  $\rho$  is the energy density,  $p$  the pressure, and  $u^a$  the 4-velocity of the fluid. In this paper we focus on polytropic equations of state

$$p = k\rho^\Gamma , \quad (4)$$

where the constant  $\Gamma$  is related to the polytropic index  $n$  according to  $\Gamma = 1 + 1/n$ . It will be assumed that  $n \geq 0$ , where the case  $n = 0$  corresponds to an incompressible fluid. In the limit  $n \rightarrow \infty$ , the polytropic equation of state (4) becomes linear and scale-invariant (it thus corresponds to the special case  $\rho_0 = 0$  in the linear equation of state,  $\rho = \rho_0 + (\eta - 1)p$ , treated in [13]).

Newtonian polytropic models have been studied for over a hundred years. Early results have been extensively described by Chandrasekhar [3], however, it is still an active area of research as exemplified by the fairly recent papers by Kimura [9] and Horedt [8]. This indicates that the Newtonian case is quite non-trivial, and the relativistic case turns out to be even more complicated, as we will demonstrate in this paper. The history of the relativistic case is also quite long. For example, Tooper [16] studied these models 35 years ago, but they have also been studied recently by, for example, deFelice *et al* [4]. Often polytropes describe low or high pressure regimes of more realistic equations of state for white dwarfs and neutron stars. These

regimes decide many of the models physical features, which therefore can be understood if the corresponding polytropic models are understood. One can also construct physically realistic composite equations of state by letting certain pressure regimes be described by polytropic equations of state. There are thus ample reasons to study models with polytropic equations of state, and it is not surprising that these models have attracted attention for a long time.

Substituting (1) into the equations of motion of the fluid,  $\nabla_a T^{ab} = 0$ , relates the gravitational potential  $\phi$  in (1) to the matter content of the spacetime according to

$$\frac{d\phi}{dp} = -\frac{1}{\rho + p} . \quad (5)$$

To facilitate the study of the gravitational field equations, we introduce various sets of bounded dimensionless variables (under scale-transformations), which regularize the gravitational field equations. Recasting the equations into regularized form on a compact state space allows us to numerically and qualitatively explore the solution space, using methods from dynamical systems theory. It is worth noticing that one can modify the approaches we introduce and apply them to large classes of equations of state. The dynamical systems are 3-dimensional in all cases. This is a great advantage since one therefore can *visualize* the compact state space and obtain a picture of the structure of the *entire* solution space for large classes of equations of state.

In the interior of a star, a mass function  $m(r)$  can be defined (see, for example, Misner & Sharp [11]). Buchdahl has derived inequalities limiting the behavior of the mass for solutions with a regular center

$$m \geq \frac{4}{3}\pi r^3 \rho , \quad (6a)$$

$$m \leq \frac{4}{3}\pi r^3 \rho_c , \quad (6b)$$

$$0 \geq 9 \left(\frac{m}{r}\right)^2 + \frac{4m}{r}(6\pi r^2 p - 1) + 4\pi r^2 p(4\pi r^2 p - 2) , \quad (6c)$$

where  $\rho_c$  is the energy density at the center of the star (see, for example, Buchdahl [1] and Hartle [7]). Alternatively, (6c) can be written as

$$\frac{m}{r} \leq \frac{2}{9} \left(1 - 6\pi r^2 p + \sqrt{1 + 6\pi r^2 p}\right) . \quad (7)$$

These inequalities are satisfied by all regular solutions, but are equalities *only* for the incompressible fluid. For such models, (6a) and (6b) characterize the regular solutions, while (6c) corresponds to a certain non-regular solution with a positive mass singularity.

A static spherically symmetric perfect fluid model has to be isolated, *i.e.*, it has to have a boundary at a finite radius, if it is to be considered as a star model. At the radius where the pressure of the fluid vanishes, the interior solution can be matched with the static Schwarzschild solution

$$ds^2 = - \left(1 - \frac{2M}{r}\right) dt^2 + \frac{dr^2}{\left(1 - \frac{2M}{r}\right)} + r^2 d\Omega^2 , \quad (8)$$

(see Schwarzschild [15]).

If (7) is evaluated at the surface of the star, defined by  $p = 0$ , we obtain

$$\frac{2M}{R} \leq \frac{8}{9} , \quad (9)$$

where  $M$  is the mass and  $R$  the radius of the star.

The outline of the paper is as follows: Section 2 constitutes the main part of the paper. In this Section, the field equations are recast into two complementary regular dynamical systems on compact state spaces. Both systems are studied numerically and qualitatively. The results are compared and various physical implications are discussed. For example, it is shown that general relativistic models have finite radii when the polytropic index  $n$  satisfies  $0 \leq n \lesssim 3.339$  and infinite radii when  $n \geq 5$ . When  $3.339 \lesssim n < 5$ , there exists a 1-parameter set of models with finite radii and a finite number, depending on  $n$ , with infinite radii. The situation thus differs from the Newtonian case where regular models have finite radii when the polytropic index satisfies  $0 \leq n < 5$ , otherwise not. In Section 3 we discuss how one can adapt the different approaches of this paper to facilitate studies of more general barotropic equations of state. We conclude in Section 4 with some remarks. In Appendix A, we indicate how the various variables were found. In Appendix B we show the relationship between our variables and the so-called Lane-Emden variables.

Throughout the paper, geometric units with  $c = G = 1$  are used, where  $c$  is the speed of light and  $G$  the gravitational constant. Roman indices,  $a, b, \dots = 0, 1, 2, 3$  denote spacetime indices.

## 2. DYNAMICAL SYSTEMS AND DYNAMICAL SYSTEMS ANALYSIS

We now present two complementary formulations adapted to the polytropic equation of state (4). In the first formulation, we introduce dimensionless variables

$$\{\Sigma, K, y\} , \quad (10)$$

according to

$$\tilde{N}^2 = y^2 K, \quad \phi' = \Sigma y, \quad r^2 = \frac{k^n P}{8\pi K} \left( \frac{1-y}{y} \right)^{1+n}, \quad y = \frac{p}{p+\rho}, \quad (11)$$

where the prime denotes differentiation with respect to the independent dimensionless spatial variable defined by the above choice of  $\tilde{N}$ . The quantity  $P$  is defined by

$$P = 1 - \Sigma^2 - K, \quad (12)$$

and can be expressed as

$$P = 8\pi K r^2 p. \quad (13)$$

Thus, the assumption of a non-negative pressure implies  $P \geq 0$ . The gauge, however, breaks down when  $P = 0$ . From (11), it follows that  $K$  is positive. We assume that the energy density  $\rho$  and the pressure  $p$  are both non-negative. This, together with the defining equation for  $y$  in (11), implies that the variable  $y$  satisfies  $0 \leq y \leq 1$ .

For a non-negative polytropic index,  $n \geq 0$ , and for a positive constant  $k$  in  $p = k\rho^{1+1/n}$ , the subset  $y = 0$  corresponds to the limit  $\rho, p \rightarrow 0$ , while the subset  $y = 1$  corresponds to the limit  $\rho, p \rightarrow \infty$ . However, one can also vary  $k$ . Setting  $k = 0 \Rightarrow p = 0$ , while  $k^{-1} = 0 \Rightarrow \rho = 0$ . These limits corresponds to  $y = 0$  and  $y = 1$ , respectively, as follows from the definition of  $y$  in (11). The same ‘‘equations of state’’ ( $p = 0$  or  $\rho = 0$ ) can be obtained from the linear equation of state,  $p = (\gamma - 1)\rho$ ;  $p = 0$  is obtained when  $\gamma = 1$  and  $\rho = 0$  is obtained when  $\gamma \rightarrow \infty$ . Thus the subsets  $y = 0$  and  $y = 1$  can be viewed as state spaces associated with the linear equation of state,  $p = (\gamma - 1)\rho$ , in the limits  $\gamma \rightarrow 1$  and  $\gamma \rightarrow \infty$ , respectively.

Integrating (5), leads to

$$e^\phi = \alpha (1 - y)^{1+n}, \quad (14)$$

where  $\alpha$  is a freely specifiable constant corresponding to the freedom of scaling the time coordinate  $t$  in the line element (1). This, in turn, reflects the freedom in specifying the value of the gravitational potential  $\phi$  at some particular value of  $r$ . Matching an interior solution with the exterior Schwarzschild solution when  $p = 0$ , however, fixes this constant to  $\alpha = \sqrt{1 - \frac{2M}{r}}$ . It is worth noting the simple relationship between the variable  $\Sigma$  and the logarithmic derivative of the gravitational potential,

$$\frac{d\phi}{d \ln r} = \frac{\Sigma}{1 - \Sigma}. \quad (15)$$

In terms of the variables  $\{\Sigma, K, u\}$ , the gravitational field equations take the form

$$\Sigma' = -yK\Sigma + \frac{1}{2}P(1 + 2y - 4y\Sigma) , \quad (16a)$$

$$K' = 2y(\Sigma^2 - P)K , \quad (16b)$$

$$y' = -(1 - \Gamma^{-1})y(1 - y)\Sigma , \quad (16c)$$

where  $\Gamma = 1 + \frac{1}{n}$ . It follows from (16b) and (16c) that  $K = 0$  and  $y = 0, 1$  are invariant subsets. By differentiating (13), we obtain

$$P' = [-\Sigma(1 + 2y + 2y\Sigma) + 2Ky]P , \quad (17)$$

which shows that  $P = 0$  is an invariant subset as well. All of these invariant subsets constitute the boundary of the physical state space, and by including them in the analysis we obtain a compact state space. For the  $K = 0$  subset, the remaining equations describe plane-symmetric polytropic models (compare with the linear equation of state discussion in [13]), and we therefore refer to this boundary subset as the plane-symmetric boundary. The state space is shown in figure 1, along with the different boundary subsets.

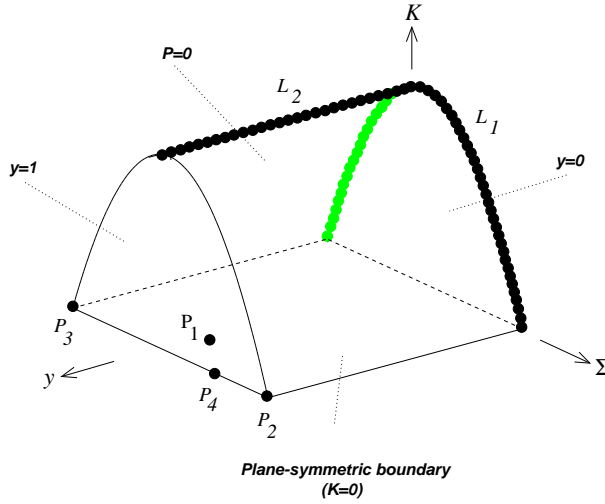


**FIG. 1.** The state space for polytropic models, together with the different boundary subsets, in terms of the variables  $\{\Sigma, y, K\}$ .

Differentiating  $r$  in (11), yields

$$r' = (1 - \Sigma)yr , \quad (18)$$

which shows that  $r$  is a monotone function for  $y \neq 0$ ,  $r \neq 0$  and  $\Sigma \neq 1$ . Together with monotone functions on the boundary subsets, this implies that all attractors are equilibrium points on the boundary subsets  $y = 0, 1$  and  $P = 0$ . The equilibrium points of (16a)-(16c) and their corresponding eigenvalues are given in Table 1. See also figure 1.

**TABLE 1.**

The equilibrium points and their stability using the variable set  $\{\Sigma, K, y\}$ .

Eq point	$\Sigma$	$K$	$y$	Eigenvalues
$L_1$	$\Sigma_s$	$1 - \Sigma_s^2$	0	$-\Sigma_s, 0, -\frac{\Sigma_s}{1+n}$
$L_2$	0	1	$y_c$	$0, -y_c, \frac{2y_c}{1+n}$
$P_1$	$\frac{2}{3}$	$\frac{1}{9}$	1	$-\frac{1}{3}, -\frac{2}{3}, \frac{2}{3(1+n)}$
$P_2$	1	0	1	$1, 2, \frac{1}{1+n}$
$P_3$	-1	0	1	$7, 2, -\frac{1}{1+n}$
$P_4$	$\frac{3}{4}$	0	1	$-\frac{7}{8}, \frac{1}{4}, \frac{3}{4(1+n)}$

The solution structure of the boundary subsets is shown in figure 2.

The equilibrium point  $P_1$  is associated with the self-similar Tolman solution, discussed in [13], in the limit  $\gamma \rightarrow \infty$  when  $p = (\gamma - 1)\rho$ . We therefore refer to this point as the Tolman point. A single orbit enters the interior state space from  $P_1$  (it is associated with the single positive eigenvalue of  $P_1$ ). We refer to this orbit as the Tolman orbit, although the corresponding exact solution is not known (except in the incompressible fluid case). An approximation of this solution near the center has been given by deFelice *et al* [4]. There originates a 2-parameter set of orbits into the interior state space from the hyperbolic source  $P_2$ . These orbits correspond to solutions with a negative mass singularity. There are no interior orbits associated with the hyperbolic saddle  $P_3$ . A 1-parameter set of orbits enters the interior state space from the hyperbolic saddle  $P_4$ . This point is associated with a self-similar plane symmetric solution discussed in [13] in the limit  $\gamma \rightarrow \infty$  when  $p = (\gamma - 1)\rho$ . The orbits coming from this point are associated with a negative mass singularity.

The  $\Sigma_s < 0$  part of the line  $L_1$  constitutes a transversally hyperbolic source from which a 2-parameter set of orbits originate. Solutions associated with these orbits start out with a negative mass. Eventually, for a sufficiently large radius  $r$ , all solutions starting out with negative mass acquire a positive mass, since the pressure is increasing with  $r$  when the mass  $m(r)$  is negative and since the pressure and energy density are assumed to be positive. The  $\Sigma_s \geq 0$  part of the line  $L_1$  constitutes the global sink. We

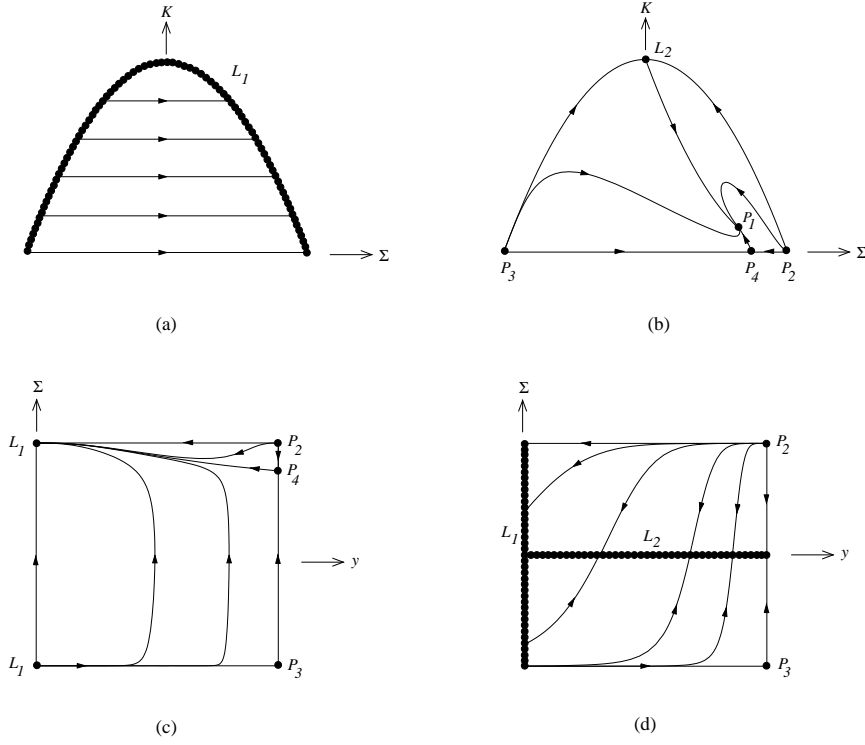


**FIG. 2.** Orbits in the boundary subsets using the variables  $\{\Sigma, K, y\}$  for (a) the boundary subset  $y = 0$ , (b) the boundary subset  $y = 1$ , (c) the plane-symmetric boundary  $K = 0$ . (d) The  $P = 0$  subset projected onto the  $K = 0$  plane.

note that the point  $\Sigma_s = 0$  on  $L_1$  is non-hyperbolic, with all three eigenvalues equal to zero. This makes it hard to analytically, as well as numerically, to resolve the dynamics in the vicinity of this point. One possibility to gain further information is to consider center-manifold theory, see Carr [2] for an introduction to the subject. We will not pursue this possibility here. Instead we will rely on an indirect discussion concerning the models radii and masses and on a second formulation, introduced below, which to a large extent resolves this problem.

Each point in the equilibrium set  $L_2$  corresponds to the flat Minkowski geometry written on spherically symmetric form (compare with the treatment in [13] where this solution was represented by a single equilibrium point). A single orbit, associated with the eigenvalue  $2y_c$ , enters the interior state space from each point of  $L_2$  when  $y_c > 0$ . The 1-parameter set



of all such orbits form a separatrix surface describing the regular subset of solutions, since the corresponding solutions all have regular centers. The individual solutions are parametrized by  $y_c$ , which in turn is determined by the value of the central energy density,  $\rho_c$ , and central pressure,  $p_c$ , according to  $y_c = \frac{p_c}{p_c + \rho_c} = \frac{k\rho_c^{1/n}}{k\rho_c^{1/n} + 1}$ . Demanding a causal star model, *i.e.*, a model where the velocity of sound of the fluid is less than or equal to the speed of light, yields the following inequality for the initial values  $y_c$  at the center of the star:

$$y_c \leq \frac{n}{1 + 2n} . \quad (19)$$

Where an orbit ends on  $L_1$  is intimately connected with the solutions total mass and radius. The ratio between the mass function  $m(r)$  and the radius  $r$ , is given by (as follows from the definition of  $m$  given by Misner & Sharp [11])

$$\frac{m}{r} = \frac{K - (1 - \Sigma)^2}{2K} . \quad (20)$$

It follows from the above equation that the static condition  $\frac{m}{r} < \frac{1}{2}$  is automatically satisfied in the interior state space. Note also that it follows that  $\Sigma > 0$  for solutions with positive mass. Evaluating (20) on  $L_1$ , where  $K = K_s = 1 - \Sigma_s^2$ , yields

$$\frac{M}{R} = \frac{\Sigma_s}{1 + \Sigma_s} . \quad (21)$$

A linear analysis shows that orbits ending at  $\Sigma_s > 0$  on  $L_1$  correspond to solutions with finite radii and masses. Orbits ending at the non-hyperbolic point  $\Sigma_s = 0$  on  $L_1$  describe solutions with infinite radii and finite masses, or masses that approach infinity slower than  $r$ .

The Buchdahl inequalities limit the possible behavior of the regular subset. Expressed in the present variables the first inequality, (6a), takes the form

$$2y(3\Sigma(1 - \Sigma) - P) \geq P , \quad (22)$$

where  $P$  is given in (12). For regular orbits, characterized by  $y_c$ , (6b) yields

$$K - (1 - \Sigma)^2 \geq KP \left( \frac{1 - y}{y} \right)^{1+n} \left( \frac{y_c}{1 - y_c} \right)^{1+n} . \quad (23)$$

The third Buchdahl inequality, (6c), leads to

$$K \geq (1 - 2\Sigma)^2 . \quad (24)$$

On the surface this inequality results in  $\Sigma_s \leq \frac{4}{5}$ .

In figure 3a,b,c some orbits in the regular subset are shown, together with the important Tolman orbit. As seen from the figures, the regular orbit on the  $y = 1$  boundary, connecting the  $y = 1$  end of  $L_2$  and the Tolman equilibrium point  $P_1$ , and the Tolman orbit play important roles for understanding the regular solutions, the latter acting not only as a boundary but also as a “skeleton” orbit for the regular set, when  $n > 0$ . The situation strongly resembles that of the linear equation of state discussed in [13]. This is not a coincidence. The regular orbit on the  $y = 1$  boundary and the Tolman orbit are completely analogous to the corresponding solutions in the linear equation of state case. As discussed earlier the  $y = 1$  set corresponds to the limit  $\gamma \rightarrow \infty$  when  $p = (\gamma - 1)\rho$ . From the figures we also see that as  $n$  increases, the orbits are pushed towards the point  $\Sigma_s = 0$  on  $L_1$  and that the maximum value of  $\Sigma_s$  for the regular solutions is closely connected with the value of  $\Sigma_s$  for the Tolman orbit.

For the incompressible fluid case,  $n = 0$ , the Tolman orbit describes a “simple” lower boundary of the regular subset and gives an upper bound  $\Sigma_s = \frac{4}{5}$  for the regular solutions when they end at  $L_1$ , see figure 3a. This upper bound is just the Buchdahl inequality (6c), which holds for all equations of state. When  $0 < n < 5$ , the situation is more complicated. In this case some regular orbits spiral around the Tolman orbit and some regular orbits end at larger  $\Sigma_s$ -values on  $L_1$  than the Tolman orbit. Nevertheless, the largest  $\Sigma_s$ -value is close to the one determined by the Tolman orbit (for which  $\Sigma_s < \frac{4}{5}$  when  $n \neq 0$ ), see figure 3b. When  $0 \leq n \leq 3$  all orbits end on  $\Sigma_s > 0$ ; when  $3 < n < 5$  a 1-parameter set of orbits end on  $\Sigma_s > 0$  and a finite number at  $\Sigma_s = 0$ , as follows from the results obtained from the second formulation below. When  $n \geq 5$ , all regular orbits spiral around the Tolman orbit and they all end at  $\Sigma_s = 0$ , see figure 3c.

Combining the above discussion with equation (15) tells us that the behavior of the gravitational potential close to the surface of a regular solution (which might be located at infinity), is to a considerable degree limited by the behavior of the gravitational potential of the non-regular solution that corresponds to the Tolman orbit. Moreover, this behavior is intimately connected with the equation of state.

An advantage of the above formulation is the regularity of the equations which makes the analysis of the center of the stars simple (compare with Rendall & Schmidt’s analysis of singular differential equations in [14]). In addition the above formulation works well when the energy density is large, even though one might be far from the center. The formulation also works well for any values of the energy density when  $n$  is small. Unfortunately, it is not well suited to deal with the low energy density limit when  $n$  is close to 3 or higher.

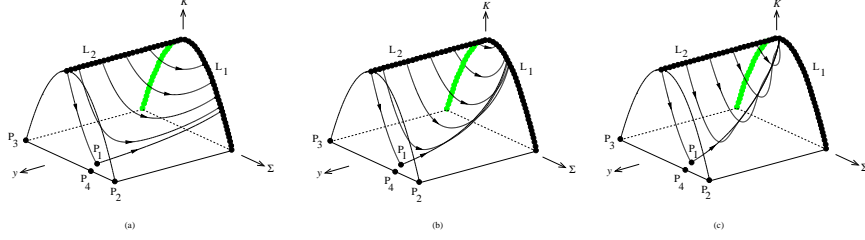


**FIG. 3.** Orbits belonging to the regular subset using the variables  $\{\Sigma, K, y\}$  for (a)  $n = 0$  (b)  $0 < n < 5$  (c)  $n \geq 5$ .

To facilitate a study of polytropic stars at low energy densities for any non-negative value  $n$ , we now present another formulation of the polytropic equations. We again choose

$$y = \frac{p}{p + \rho} \quad (25)$$

as a variable, but make a non-linear transformation of  $K$  and  $\Sigma$  to a new set of dimensionless variables  $U$  and  $V$  (see Appendix A). We first introduce the Newtonian homology invariants  $u, v$  (see, for example, Kimura [9])

$$u = \frac{4\pi r^3 \rho}{m}, \quad v = \frac{m\rho}{rp}, \quad (26)$$

and then define the variables  $U$  and  $V$  according to

$$U = \frac{u}{1+u} = \frac{4\pi r^2 \rho}{4\pi r^2 \rho + m/r}, \quad V = \frac{v}{1+v} = \frac{m/r}{m/r + p/\rho}. \quad (27)$$

The assumptions of positive energy density, pressure, and mass lead to the inequalities  $0 < U < 1$  and  $0 < V < 1$ . It follows that

$$r^2 = \frac{k^n UV}{4\pi(1-U)(1-V)} \left( \frac{1-y}{y} \right)^{n-1}, \quad (28a)$$

$$e^\phi = \alpha (1-y)^{1+n}. \quad (28b)$$

We now choose a new independent variable such that the function  $\tilde{N}$  takes the form

$$\tilde{N}^2 = (1-y)^3(1-V)(1-U)^2 F r^{-2}, \quad F = (1-V)(1-y) - 2yV, \quad (29)$$

where  $r^2$  has been given in equation (28a). We thereby incorporate the assumptions of positive energy density, pressure, and mass in the gauge, which becomes ill-defined when these requirements are not satisfied.

In terms of the variables  $\{U, V, y\}$ , the gravitational field equations, which are again completely regular, takes the form

$$U' = U(1 - U) [(1 - y)(3 - 4U)F - \Gamma^{-1}G] , \quad (30a)$$

$$V' = V(1 - V) [(1 - y)(2U - 1)F + (1 - \Gamma^{-1})G] , \quad (30b)$$

$$y' = -(1 - \Gamma^{-1})y(1 - y)G , \quad (30c)$$

where

$$G = V [(1 - U)(1 - y) + yU] , \quad (31)$$

and where  $\Gamma = 1 + 1/n$ . The prime denotes differentiation with respect to the independent variable, defined by (29). By including the invariant subsets  $U = 0, 1, V = 0, 1, y = 0, 1$  of (30a)-(30c) we obtain a compact state space. These subsets can be interpreted in terms of limits of  $\frac{m}{r}, \frac{p}{\rho} = k\rho^{1/n}$  and  $\rho r^2$ . The incorporation of the positive pressure, energy density and mass conditions in the gauge has led to that we now have invariant subsets corresponding to setting these quantities to zero. From (30c) it follows that  $y$  is a monotonically decreasing function, and all orbits in the interior of the state space approach the  $y = 0$  subset. The equilibrium points of (30a)-(30c) and their eigenvalues are given in Table 2.

Before continuing the discussion of the system (30a)-(30c), it is of interest to consider the Newtonian equations in terms of the variables  $\{U, V, y\}$ . These are given by:

$$U' = U(1 - U) [(3 - 4U)(1 - V) - \Gamma^{-1}V(1 - U)] , \quad (32a)$$

$$V' = V(1 - V) [(2U - 1)(1 - V) + (1 - \Gamma^{-1})V(1 - U)] , \quad (32b)$$

$$y' = -(1 - \Gamma^{-1})y(1 - y)V(1 - U) . \quad (32c)$$

Note that the non-homologous variable  $y$  is decoupled in the above system, leaving a coupled 2-dimensional reduced homology invariant set of equations. The reduced homology-invariant set of equations is identical to the  $y = 0$  subset of the relativistic equations (30a) and (30b). We therefore refer to the  $y = 0$  subset as the Newtonian subset. Taking the Newtonian limit of all the relativistic equations (30a)-(30c) thus corresponds to letting  $y$  go to zero (except in the equation for  $y$  where one must be more careful). Hence we obtain the Newtonian homology-invariant equations as the ‘‘low pressure’’ boundary of the relativistic state space. It is worth noting that the projection of the Newtonian orbits onto the subset  $y = 0$ , coincides with the orbits on the same subset, because of the decoupling of the  $y$ -equation.

We now return to the relativistic case. We are considering static models and thus the inequality  $\frac{2m}{r} < 1$  must be satisfied. Solving for  $\frac{m}{r}$  in equation (27) leads to the expression

$$\frac{m}{r} = \left( \frac{V}{1-V} \right) \left( \frac{y}{1-y} \right). \quad (33)$$

Inserting this into  $\frac{2m}{r} < 1$  yields the inequality

$$\frac{1-y}{1+y} > V. \quad (34)$$

The state space, together with the intersection of the “static surface”  $(1+y)V - (1-y) = 0$  with the  $U = 0$  and  $U = 1$  boundary subsets, is depicted in figure 4. Note that the static surface “forces” the static solutions away from the line  $L_5$  and the point  $P_3$ , which thus are of little interest for the static solutions.

Expressed in the present variables, the first Buchdahl inequality (6a) leads to

$$U \leq \frac{3}{4}. \quad (35)$$

This inequality “forces” the regular subset away from  $P_5$ . Inserting equations (33) and  $6\pi r^2 p = \frac{3}{2}UVy^2(1-U)^{-1}(1-V)^{-1}(1-y)^{-2}$  into (6b) leads to a complicated expression, which we will not give. For regular orbits characterized by  $y_c$ , equation (6b) yields

$$\left( \frac{y}{y_c} \right) \left( \frac{1-y_c}{1-y} \right) \leq \frac{1}{3} \left( \frac{U}{1-U} \right). \quad (36)$$

A disadvantage with the present formulation is that the entire  $y = 1$  subset, in the  $\{\Sigma, K, y\}$ -formulation (see figure 2(b)), has been “crushed” into the line  $L_3$ . We also note from Table 2 that this line is non-hyperbolic, with three zero eigenvalues. This means that studying the dynamics in a neighborhood of this line can be quite complicated. By relying on results from the  $\{\Sigma, K, y\}$ -formulation, we can circumvent most of these problems. Although the previous formulation gives a better picture of what happens at large energy densities, the present formulation gives a better picture of the low energy density regime. The two formulations are thus complementary.

When discussing the solution structure using the  $\{\Sigma, K, y\}$ -formulation, we emphasized the importance of certain special orbits, for example, the Tolman orbit. Thus it is important to identify this orbit in the present formulation. The first step in order to do this is to identify where the Tolman

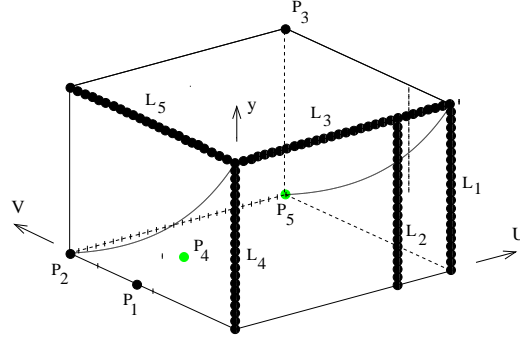


**FIG. 4.** The structure of the state space using the variables  $\{U, V, y\}$ . The curves indicated on the  $U = 0$  and  $U = 1$  subsets are the intersections between these subsets and the “static surface”  $(1 + y)V - (1 - y) = 0$ .

**TABLE 2.**

The equilibrium points and their stability using the variables  $\{U, V, y\}$ .  
Here  $\lambda_3 = -\frac{n-1}{(n-2)(1+3n)}$  and  $a = 1 + 22n - 7n^2$

Eq. point	$U$	$V$	$y$	Eigenvalues	Restrictions
$L_1$	1	0	$y_0$	$(1 - y_0)^2, (1 - y_0)^2, 0$	
$L_2$	$\frac{3}{4}$	0	$y_c$	$-\frac{3}{4}(1 - y_c)^2, \frac{1}{2}(1 - y_c)^2, 0$	
$L_3$	$U_0$	0	1	0, 0, 0	
$L_4$	0	0	$y_0$	$3(1 - y_0)^2, -(1 - y_0)^2, 0$	–
$L_5$	0	$V_0$	1	0, 0, 0	–
$L_6$	$U_0$	1	0	0, $-(1 - U_0), -(1 - U_0)$	$n = 0$
$P_1$	0	$\frac{1+n}{2+n}$	0	$-\frac{n-3}{2+n}, \frac{1}{2+n}, -\frac{1}{2+n}$	–
$P_2$	0	1	0	$-\frac{n}{1+n}, -\frac{1}{1+n}, -\frac{1}{1+n}$	–
$P_3$	1	1	1	$\frac{n}{1+n}, -\frac{1}{1+n}, \frac{1}{1+n}$	–
$P_4$	$\frac{n-3}{2(n-2)}$	$\frac{2(1+n)}{1+3n}$	0	$\frac{-\lambda_3}{4}(5 - n \pm \sqrt{a}), \lambda_3$	$n > 3$
$P_5$	1	1	0	0, 0, 0	–

point from which it originates is located. This point corresponds to a point characterized by  $U = (3 + n)/2(2 + n)$  and  $V = 0$  in the equilibrium set  $L_3$ , as can be seen using the variable transformations given in Appendix A. From these transformations one also sees that the “plane-symmetric” point  $P_4$ , in the  $\{\Sigma, K, y\}$ -formulation, corresponds to the equilibrium point  $U = 0, V = 0, y = 1$ , *i.e.*, the intersection of the three lines  $L_3, L_4$  and  $L_5$ . We know from the previous analysis that this latter point is associated

with a 1-parameter set of solutions originating from it and that these solutions start out with negative mass. Transforming from the  $\{\Sigma, K\}$ -picture to the  $\{U, V\}$ -picture shows that the 1-parameter set of orbits starts from  $U = 0, V = 0, y = 1$  entering the “negative mass part” of the state space outside the cube. They eventually end at  $L_1$  when the total mass becomes zero. This line is just an artifact of the gauge choice. Using the previous formulation one can continue the solutions through  $L_1$  into the interior “positive mass part” of the cube. The situation is analogous to that encountered in the diagonal homothetic approach for self-similar spherically symmetric models when one matches the spatially self-similar part with the timelike self-similar part, as described in Goliath *et al* [5], [6]. The 2-parameter set of orbits associated with  $P_2$  in the  $\{\Sigma, K, y\}$ -formulation starts from  $L_3$  and enters into the negative mass regime of the state space outside of the cube, but eventually pass through  $L_1$  into the interior state space, in the  $\{U, V, y\}$ -formulation. The 2-parameter set of orbits associated with the  $\Sigma_s < 0$  part of  $L_1$  (in the  $\{\Sigma, K, y\}$ -formulation) start from  $L_1$  (in the  $\{U, V, y\}$ -formulation) entering the exterior state space and eventually pass through  $L_1$  into the interior state space.

In the  $\{U, V, y\}$ -formulation, all regular solutions start from the line  $L_2$ , and are again parametrized by  $y_c$ . For  $n = 3$ , the equilibrium point  $P_4$  enters the state space through the point  $P_1$ , changing the stability of  $P_1$  from a source to a saddle. As  $n$  increases,  $P_4$  first changes from a node to a focus and then, at  $n = 5$ , to a center in the Newtonian subset. When  $n > 5$   $P_4$  is a local sink of the full state space. The point  $P_4$  corresponds to a special singular Newtonian solution.

To be able to determine if an orbit corresponds to a model with finite mass or radius, it is useful to consider equation (28a) and the following equations

$$r' = (1 - y)(1 - U)Fr, \quad (37a)$$

$$m' = \frac{UV^2y^2Fm}{(1 - V)^2(1 - y)}, \quad (37b)$$

$$m^2 = \frac{k^n UV^3}{4\pi(1 - U)(1 - V)^3} \left( \frac{y}{1 - y} \right)^{3-n}, \quad (37c)$$

where  $F = (1 - V)(1 - y) - 2yV$ .

The radius of a model is definitely infinite if  $r'$  does not approach zero as  $\lambda \rightarrow +\infty$ . The corresponding statement holds for the mass,  $m$ , as well. The variable  $y$  is monotonically decreasing and all orbits end at the Newtonian boundary subset. This, in conjunction with the stability of the equilibrium points given in Table 2, implies the following: *Only* orbits that end at the hyperbolic sink  $P_2$  (or the equilibrium set  $L_6$  for  $n = 0$ ) correspond to star models with finite radii. These models also have finite mass. If an orbit

ends at one of the other possible equilibrium points,  $P_1$  or  $P_4$ , a model with infinite radius is obtained. If it ends at  $P_1$  it yields a model with finite mass and if it ends at  $P_4$  the corresponding model has infinite mass. This follows from a linear analysis of equations (28a) and (37a)-(37c). Note that the above statements also hold for the Newtonian models, described by the  $y = 0$  subset and the decoupled  $y$ -equation (32c).

We now consider the Newtonian subset  $y = 0$ , since this subset is of great importance also for relativistic stars.

### 2.1. The Newtonian subset

Newtonian polytropic stars have been studied extensively in the literature. Chandrasekhar [3] primarily used the Lane-Emden approach, while the homology-invariant variables  $\{u, v\}$  were used by, for example, Kimura [9] and Horedt [8]. Both Kimura as well as Horedt used dynamical systems techniques in their investigations, but since they did not use bounded variables, their state spaces were not compact.

From these previous analyses, however, it is known that regular Newtonian solutions exist for all  $n \geq 0$ , and that when  $0 \leq n < 5$  they give rise to finite star models while  $n \geq 5$  lead to infinite regular models. These results are easily obtained using the variables  $\{U, V\}$ . The solution structure of the Newtonian subset for different values of  $n$  is shown in figure 5. The orbit corresponding to the regular solution (called the E-solution in the literature) starts at  $y = 0$  on  $L_2$ , and we refer to it as the regular Newtonian orbit. As indicated in the discussion above, the equilibrium point where the orbit ends, depends on the value of  $n$ . For the solvable incompressible fluid case  $n = 0$ , the regular orbit is characterized by  $U = \frac{3}{4}$ , and end on the corresponding point on  $L_6$ . For  $0 < n < 5$ , it ends at  $P_2$ . Thus, for these values of  $n$ , the radius and mass of the star model are finite. We also note that for  $0 \leq n \leq 3$  there exists a monotone function,

$$Z = \frac{UV^3}{(1-U)(1-V)^3}, \quad (38)$$

which satisfies

$$\frac{Z'}{Z} = 2nU(1-V) + (3-n)V(1-U). \quad (39)$$

For  $n = 5$ , however, the regular Newtonian orbit ends at  $P_1$ , and thus corresponds to a model with infinite radius but with finite mass. Note that for  $n = 5$ , the point  $P_4$  is a center. This is not just a feature of the linear analysis. The case  $n = 5$  is exactly solvable, see, for example, Chandrasekhar [3], so there exists an integral, which in our variables takes



the form

$$D(1-U)^{3/2}(1-V)^{5/2} = 6\sqrt{UV}H, \quad (40)$$

with

$$H = 2(1-U)(4V-3)^2 + 4UV(1-V) - 3(1-U)(1-V)^2, \quad (41)$$

where  $D$  is a constant. Setting  $D = 0$  yields the regular orbit. Negative values of  $D$  parametrizes the closed orbits around  $P_4$ . These orbits correspond to non-regular models with infinite radii. The orbits that end at  $P_2$  are parametrized by the positive values of  $D$ . For  $n > 5$  all orbits end at  $P_4$ , giving rise to models with infinite radii and masses.

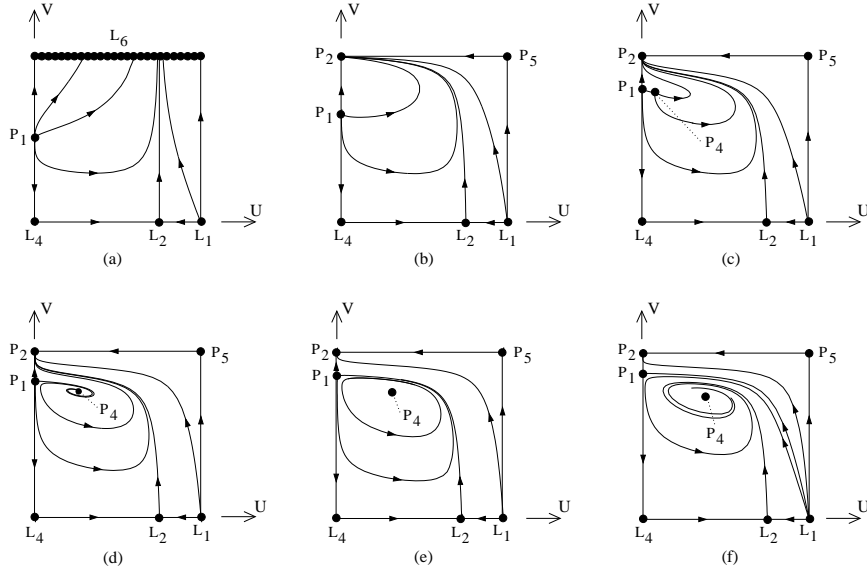


**FIG. 5.** Orbits in the Newtonian subset  $y = 0$  in terms of the variables  $\{U, V\}$  for (a)  $n = 0$ , (b)  $0 < n \leq 3$ , (c)  $3 < n \leq (11 + 8\sqrt{2})/7$ , (d)  $(11 + 8\sqrt{2})/7 < n < 5$ , (e)  $n = 5$ , and (f)  $n > 5$ .

## 2.2. Regular relativistic stars

The dynamics of the relativistic case is much more complicated than in the Newtonian case. In contrast to the Newtonian case, a projection of the orbits onto the plane  $y = 0$  does not coincide with the orbits in the  $y = 0$  subset, since the equation for  $y$  is not decoupled. The regular subset is a

1-parameter set of orbits starting from  $L_2$ , defining a separatrix surface in state space. In the interior of state space, the Tolman orbit constitutes the boundary of this separatrix surface. Since  $y$  is a monotone function, all orbits end at the Newtonian boundary. We will now discuss the behavior of the orbits in the regular subset for different values of  $n$ .

### 2.3. The incompressible fluid models

The behavior of a relativistic incompressible fluid ( $n = 0$ ) is quite reminiscent of the Newtonian case. All orbits in the regular subset lie in the plane  $U = \frac{3}{4}$ , and thus end at  $U = \frac{3}{4}$  on  $L_6$ . The regular subset projected on the Newtonian subset  $y = 0$  is shown in figure 6a.

We note that it is possible to solve the equations exactly for the incompressible fluid, just as in the Newtonian case (see, for example, Tooper [16], who uses the relativistic Lane-Emden equation).

### 2.4. Models with $0 < n \leq 3$

For models with  $0 < n \leq 3$ , Table 2 shows that  $P_2$  is a hyperbolic sink. The fact that  $y$  is a monotone function that pushes all orbits down to the Newtonian subset, in conjunction with the existence of the monotone function (38) in the Newtonian subset for  $0 \leq n \leq 3$ , implies that  $P_2$  is, in fact, the global sink and *all* orbits end at this point. Therefore the radii and masses of all regular stars are finite when  $0 < n \leq 3$ . This is consistent with a theorem given by Makino [10], which in the present context states that the radius of a regular model is finite when  $1 < n < 3$  (see Theorem 1, p 60 in [10]).

The regular subset projected onto the plane  $y = 0$  is shown in figure 6b, where the regular Newtonian orbit is shown as a dashed line. Also shown is the Tolman orbit, starting from  $L_3$ . Orbits characterized by an initial value of  $y_c$  close to unity, start out close to  $L_3$ , and then follow the Tolman orbit closely. Note that the separatrix surface formed by the regular subset of orbits folds over itself.

### 2.5. Models with $3 < n < 5$

For  $3 < n < 5$ , the point  $P_2$  is still the only sink, and the majority of orbits will end at  $P_2$ . Hence most regular orbits are expected to end there too, but there are other possibilities for where the orbits of the regular subset can end. There exists a 1-parameter set of orbits that end at  $P_1$ , and thus gives rise to a separatrix surface in state space. The corresponding solutions have finite masses but infinite radii. The boundary of the separatrix surface associated with  $P_1$  is described by an orbit in the  $U = 0$  submanifold, an orbit in the Newtonian subset  $y = 0$  connecting the point  $P_1$  with  $P_4$ , and a relativistic orbit ending at  $P_4$ . The solution corresponding to this latter orbit have both infinite mass and radius. If the “regular”

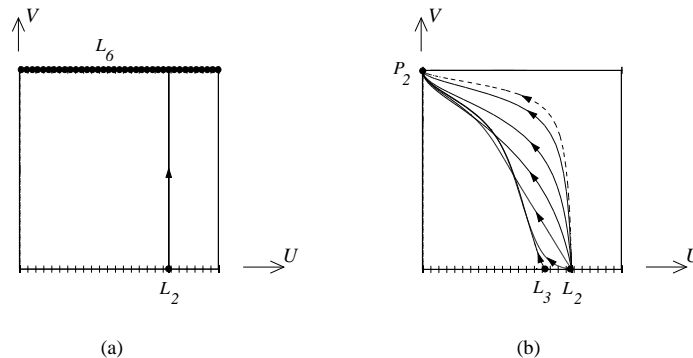


**FIG. 6.** Orbits belonging to the regular subset and the Tolman orbit using the variables  $\{U, V, y\}$  for (a) the incompressible fluid,  $n = 0$ , and (b)  $0 < n \leq 3$ . The Newtonian orbit corresponds to the dashed line.

separatrix surface intersects this separatrix surface or its boundary orbit in the interior state space, there will be an orbit, ending at  $P_1$  or at  $P_4$ , respectively, instead of  $P_2$ . The two surfaces could, of course, intersect each other several times, resulting in several infinite solutions. What actually happens depends on the value of  $n$ , as discussed below.

We have been forced to rely on numerical simulations in order to decide where the orbits of the regular subset actually end. To systematically explore if there are regular orbits that end at  $P_1$  or  $P_4$ , we proceed as follows. We first note that when  $3 < n < 5$ , there always exist a constant  $c_1 > 0$ , such that all orbits with  $y_c < c_1$  end at  $P_2$ . This follows from our numerical investigation, but is also a consequence of Theorem 4 on p 994 in Rendall & Schmidt [14] (see also Theorem 2 p 64 in Makino [10]), which states the following in the present context. Any relativistic polytropic model with  $1 < n < 5$  and central density  $\rho_c$  has finite radius if  $k$  is sufficiently small. Since  $y_c = \frac{p_c}{p_c + \rho_c} = \frac{k\rho_c^{1/n}}{k\rho_c^{1/n} + 1}$ , this means that models with sufficiently small  $y_c$  lead to finite stars. Since  $y$  is a monotone function, the intersections of the separatrix surfaces with a plane  $y = c_2$  are curves. Hence, an intersection of the separatrix surfaces corresponds to an intersection of the two corresponding curves in the plane  $y = c_2 > c_1$ . To visualize the intersections of the two separatrix surfaces for a given  $n$ , we thus first ensure, numerically, that all orbits with  $y_c \leq c_2$ , where  $c_2 > 0$  is chosen to be some convenient value, end at  $P_2$ . We then numerically calculate the separatrix surfaces and plot their intersection with the plane  $y = c_2$ .

Numerical simulations indicate that all regular orbits end at  $P_2$  for  $3 < n \lesssim 3.339$ , and all regular models are thus finite for this range of  $n$ , see

figure 7a. The first time the two separatrix surfaces intersect each other is when  $n \approx 3.339$ , see figure 7b. Thus there is a single regular orbit ending at  $P_1$ , corresponding to a solution with finite mass and infinite radius. All other regular orbits end at  $P_2$ , giving rise to models with finite radii and masses. When  $n$  is larger than the above value there is always at least one separatrix intersection with a “ $P_1$ -orbit” and there is at least one solution with finite mass and infinite radius.

In figure 7c the intersection between the two separatrix surfaces for  $n = 3.6$  with the plane  $y = c_2 = 0.1$  is shown. The single point of intersection of the two curves shows that there exists a single infinite solution. For  $n = 4.1$ , the result is shown in figure 7d. We note that there are several infinite solutions, but they are all isolated, and this is typical. Intersections always seem to take place at isolated points. The behavior of the regular subset projected onto the Newtonian subset is shown in figure 8a for  $3 < n \lesssim 3.339$  and in figure 8b for  $3.339 \lesssim n < 5$ . One should note that as  $n$  approaches 5, the behavior of the regular subset becomes more and more complicated.

The boundary orbit of the  $P_1$ -separatrix surface, corresponding to the  $P_4$  orbit, may also intersect the regular separatrix surface. This happens when  $n \approx 3.357$  and  $n \approx 4.414$ . In these cases one obtains solutions with infinite masses and radii.

The Tolman orbit, *i.e.*, the boundary of the regular subset, also intersects the  $P_1$ -separatrix surface. This happens at an increasing rate as  $n$  approaches 5. The first five values of  $n$  when this happens are 3.673, 3.939, 4.105, 4.221 and 4.309.

The lowest initial value of  $y_c$  leading to an infinite model decreases towards zero when  $n$  increases towards 5. For  $n = 5$  it coincides with  $y_c = 0$ . The relativistic 3-dimensional state space thus sheds light on the appearance of an infinite Newtonian star for  $n = 5$ .

It is worth noting that the appearance of infinite solutions is a source of considerable problems in the Lane-Emden approach.

## 2.6. Models with $n = 5$

When  $n = 5$ , the separatrix surface that ends at the equilibrium point  $P_1$  completely encloses the regular subset of orbits. This makes it impossible for any regular orbit to end at  $P_2$ . The Newtonian regular orbit is the lower boundary of the separatrix surface and thus end at  $P_1$ , while all relativistic regular orbits are forced towards  $P_4$  and the closed orbits surrounding  $P_4$ , in the Newtonian subset  $y = 0$ . All relativistic regular models therefore have infinite radii and masses. The enclosing separatrix surface is shown in figure 9a, and the projection of the regular subset and the Tolman orbit onto the Newtonian subset  $y = 0$  is shown in figure 9b.

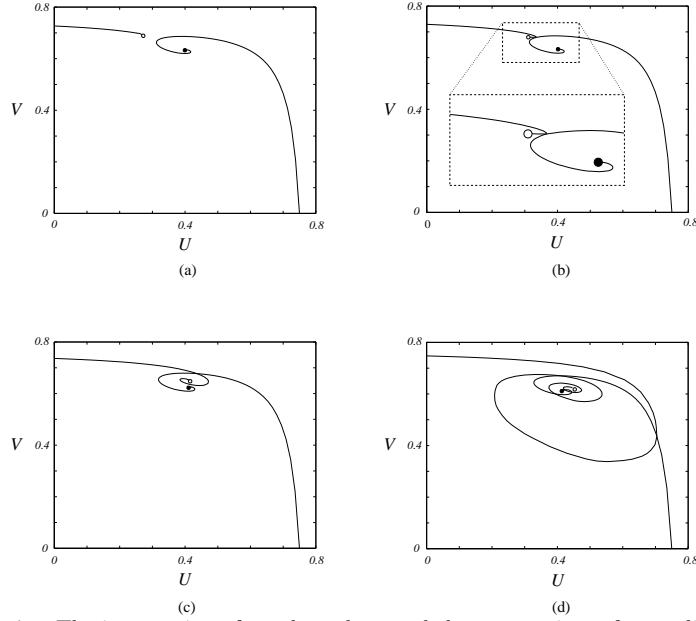


**FIG. 7.** The intersection of regular subset and the separatrix surface ending at the equilibrium point  $P_1$  in the plane  $y = 0.1$ , for (a)  $n = 3.1$ , (b)  $n \approx 3.339$ , (c)  $n = 3.6$ , and (d)  $n = 4.1$ .

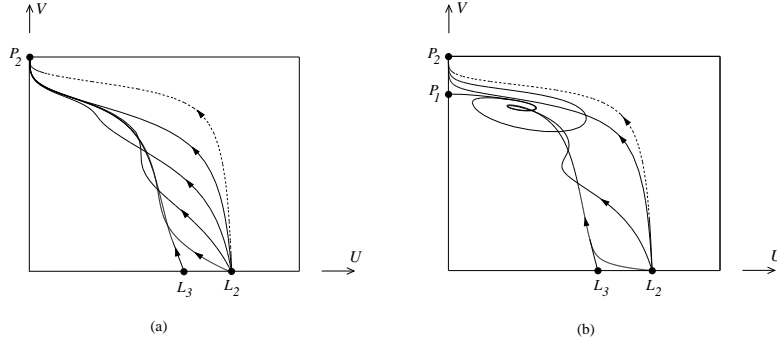


**FIG. 8.** Orbits belonging to the regular subset and the Tolman orbit using the variables  $\{U, V, y\}$ , for (a)  $3 < n \lesssim 3.339$  and (b)  $3.339 \lesssim n < 5$ .

### 2.7. Models with $n > 5$

When  $n > 5$ , the situation is similar to the case  $n = 5$ . The separatrix surface associated with  $P_1$  now encloses *all* regular orbits (including the regular Newtonian orbit) and all regular orbits end at the sink  $P_4$ . Hence

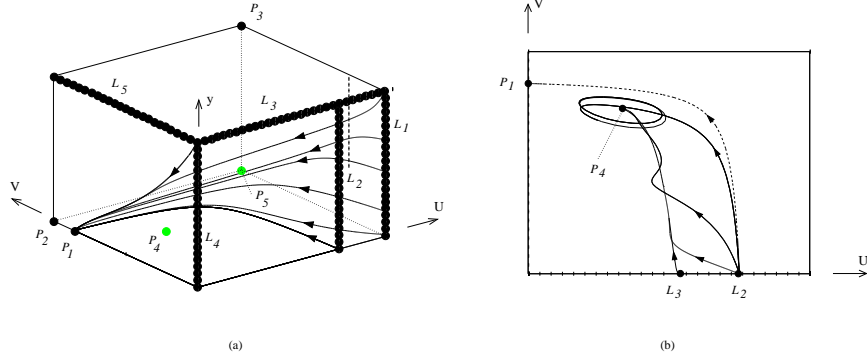


**FIG. 9.** (a) The behavior of the separatrix surface ending at the equilibrium point  $P_1$  that excludes any finite polytropic stars with  $n = 5$ . (b) Orbits in the regular subset and the Tolman orbit projected onto the Newtonian subset  $y = 0$ .

all polytropic models with  $n > 5$ , Newtonian and relativistic, have infinite radii and masses. The enclosing separatrix surface associated with  $P_1$  is shown in figure 10a, and the projection of the regular subset and the Tolman orbit onto  $y = 0$  is shown in figure 10b.

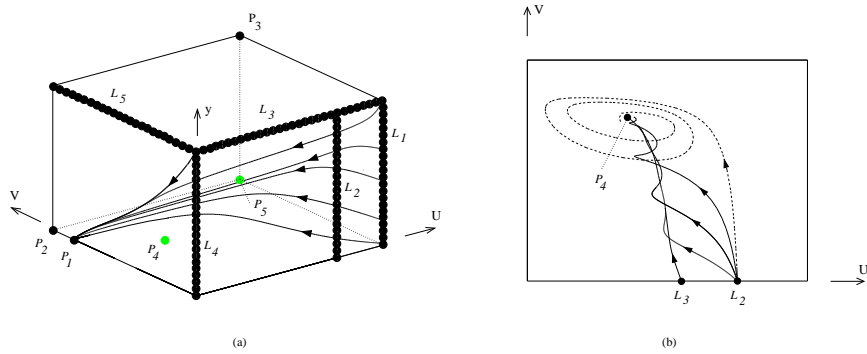


**FIG. 10.** (a) The behavior of the separatrix surface ending at the equilibrium point  $P_1$  that excludes any finite polytropic stars with  $n > 5$ . (b) The orbits of the regular subset and the Tolman orbit projected onto the Newtonian subset  $y = 0$ .

### 3. COMMENTS ON THE GENERAL BAROTROPIC EQUATION OF STATE

**TABLE 3.**

The functional form of  $1 - \Gamma^{-1}$  for some common equations of state.  
Here  $\rho_m$  is the rest mass density and  $\bar{\eta} = \bar{\Gamma}/(1 - \bar{\Gamma})$ .

Type	Eq. of state	$1 - \Gamma^{-1}$
Incompressible	$\rho = \text{const}$	1
Scale-invariant	$p \propto \rho$	0
Polytrope	$p \propto \rho^{1+1/n}$	$(1 + n)^{-1}$
Linear	$\rho = (\eta - 1)p + \rho_0$	$(1 - \eta y)/(1 - y)$
Relativistic polytrope	$p = k\rho_m^{\bar{\Gamma}}, \quad \rho = \rho_m + p/(\bar{\Gamma} - 1)$	$(1 - \bar{\eta}y)/[\bar{\eta}(1 - y)]$

In this section we address the issue whether it is possible to use, or at least modify, the above formulations, in order to understand models with other barotropic equations of state.

In general, a barotropic equation of state,  $p = p(\rho)$ , leads to that

$$\Gamma = \frac{d \ln p}{d \ln \rho} \quad (42)$$

is a function of  $y$ . For a given  $\Gamma(y)$ , one can parametrize the equation of state in terms of  $y$  as follows:

$$\rho = \rho_0 \exp \left( \int \frac{dy}{(\Gamma(y) - 1)y(1 - y)} \right), \quad (43a)$$

$$p = p_0 \exp \left( \int \frac{\Gamma(y)dy}{(\Gamma(y) - 1)y(1 - y)} \right). \quad (43c)$$

The parametrization, however, might break down, but in such cases one can in principle obtain the equation of state in a piece-wise manner, except when  $\Gamma = 1$  everywhere. This latter situation corresponds to a linear scale-invariant equation of state,  $p = (\gamma - 1)\rho$ , easily treated with other methods, see, for example [13].

To obtain a formulation for non-polytropic equations of state, one has to replace the constant  $\Gamma$  in the equations in the previous section with the function  $\Gamma(y)$ . The functional form of the factor  $1 - \Gamma^{-1}$  for some common equations of state is given in Table 3.

It should be pointed out that in general  $y$  is not a monotone single-valued function of  $p$ . Several values of  $p$  and  $\rho$  might correspond to the same value of  $y$ . This can be visualized as follows: First note that there is a one-to-one correspondence between  $y$  and  $\frac{\rho}{p}$  since  $y = \frac{1}{1 + (\rho/p)}$ . Then plot the equation of state in a  $\rho$ - $p$  diagram. The slope of a straight line from the origin determines  $\frac{\rho}{p}$  and therefore  $y$ . From this construction one can deduce the functional properties of  $y$  as a function of  $p$  or  $\rho$ . If a straight

line intersects the equation of state curve several times, then several values of  $p$  and  $\rho$  correspond to the same value of  $y$ . This feature is of course encoded in the above equations. If this situation occurs, then  $y$  is not a monotone function and  $1 - \Gamma(y)^{-1}$  becomes zero for one or several values of  $y$  in the interval  $0 < y < 1$ . For these values of  $y$  one obtains invariant subsets described by the scale-invariant linear equation of state. If there are only a few zeroes of  $1 - \Gamma^{-1}$ , one may match orbits and obtain the complete solution.

It is only possible to obtain  $\Gamma$  as a function of  $y$  explicitly for a limited set of equations of state. Because of these difficulties, a better strategy for most equations of state, particularly if  $1 - \Gamma^{-1}$  has several zeroes, is to change from  $y$  to another variable  $z = z(y)$ , that is a monotone function of  $p$ , and treat  $y$  as a function of  $z$  in the equations and if necessary choose a new independent variable. Simple examples of new variables are, for example,  $p$ , some simple function of  $e^\phi$  (like the redshift), or, if one wants a bounded variable, for example,  $z = \frac{p}{a^2+p}$ ,  $z = \frac{e^\phi}{a^2+e^\phi}$ , where  $a^2$  is some arbitrary constant with suitable dimension, but preferably associated with the equation of state of interest. It might happen that one obtains new boundaries replacing, for example, the  $y = 1$  boundary for the physical interesting part. This is exemplified by the linear equation of state, for which  $1 - \Gamma^{-1} = \frac{1-\eta y}{1-y}$  and the relativistic polytrope, for which  $1 - \Gamma^{-1} = (1 - \bar{\eta}y)/\bar{\eta}(1 - y)$ . In these cases one obtains a boundary at  $y = \frac{1}{\eta}$  and  $y = \frac{1}{\bar{\eta}}$  respectively, instead of at  $y = 1$ . Note that for the system to be useful, one requires that the equations are differentiable of at least order  $C^1$  on the entire physical state space and its boundaries.

To exemplify that one can use the polytropic formulations for other equations of state, we will first consider the linear equation of state and make comparisons with the approach described in [13]. In the  $\{\Sigma, K, y\}$ -formulation one only needs to replace  $1 - y$  with  $1 - \eta y$  in the equation for  $y$ . Hence  $y = \eta^{-1} < 1$  replaces the boundary subset  $y = 1$  and the physically interesting region is characterized by  $y \leq \eta^{-1} \leq 1$ . The resulting dynamical system is completely regular on the physical state space and its boundaries.

In [13] the state space allowed orbits corresponding to solutions with negative pressure. This is not the case now. We have incorporated the positive pressure condition in the gauge and we therefore now have an invariant subset corresponding to setting  $p$  to zero. Instead of ending at a non-invariant surface of zero pressure, as in [13], the regular orbits now end at  $\Sigma_s s > 0$  on  $L_1$ , since all regular solutions have finite radii and masses, see [13]. In addition, all regular solutions now start from a line of equilibrium points  $L_2$ , while in [13] they all started from a single isolated equilibrium point.



For a linear equation of state the  $\{U, V, y\}$ -formulation yields the following equations:

$$U' = U(1 - U) [(1 - y)(3 - 4U)F - \Gamma^{-1}G] , \quad (44a)$$

$$V' = V(1 - V) [(1 - y)(2U - 1)F + (1 - \Gamma^{-1})G] , \quad (44b)$$

$$y' = -y(1 - \eta y)G , \quad (44c)$$

where

$$F = (1 - V)(1 - y) - 2yV , \quad (45a)$$

$$G = V[(1 - U)(1 - y) + yU] , \quad (45b)$$

and where

$$1 - \Gamma^{-1} = \frac{1 - \eta y}{1 - y} . \quad (46)$$

The expression  $(1 - y)^{-1}$  occurs as a factor in the above dynamical system, except when  $\eta = 1$  and  $\Gamma^{-1} = 0$ . This case corresponds to an incompressible fluid and can thus be obtained by setting  $n = 0$  in the polytropic equation of state. For  $\eta > 1$ ,  $y = \eta^{-1} < 1$  replaces  $y = 1$  as the boundary subset of the physically interesting region. Thus  $y \leq \eta^{-1} < 1$ , and this implies that  $1 - y > 0$ . Hence the above system is completely regular on the physical state space and its boundaries. If one is so inclined, one can change the independent variable with a factor of  $(1 - y)$  so that one obtains polynomial equations. Note that  $y$  is a monotone function in the physically interesting region for this case and thus there is no need to change to another variable  $z = z(y)$ .

Solutions that start with negative mass enter the interior state space through a line of equilibrium points, which did not exist in the linear equation of state treatment in [13]. In addition, all regular solutions start from a line of equilibrium points, while they all started from a single isolated equilibrium point in [13]. Moreover, instead of ending at a surface of vanishing pressure as in [13], they all end at the equilibrium point  $P_2$  on the  $y = 0$  subset.

The pictures are thus quite different, but one can extract all interesting physical information about, for example, the regular solutions from any of the above formulations. However, note that it is easier to extract information about total masses and radii using the formulation given in [13].

The relativistic polytropic equation of state

$$p = k\rho_m^{\bar{\Gamma}} , \quad \rho = \rho_m + \frac{p}{\bar{\Gamma} - 1} , \quad (47)$$

where  $\rho_m$  is the rest mass density and  $\rho$  the energy density, provides another example where the previous formulations works well. For this equation of state the polytropic exponent  $\bar{\Gamma}$  coincides with the adiabatic index  $\Gamma_a$

$$\Gamma_a = \left( \frac{\rho + p}{p} \right) \frac{dp}{d\rho}, \quad (48)$$

which is not the case for  $\Gamma$  in  $p = k\rho^\Gamma$ . This equation of state asymptotically approach the linear equation of state  $p = (\bar{\Gamma} - 1)\rho$  when  $p, \rho \rightarrow \infty$  and the polytropic equation of state  $p = k\rho^{\bar{\Gamma}}$  when  $p, \rho \rightarrow 0$ . Hence, the  $y = 1$  boundary is replaced with a boundary  $y = \frac{1}{\bar{\Gamma}}$ , described by a scale-invariant linear equation of state. The  $y = 0$  boundary is just the Newtonian polytropic boundary discussed previously.

#### 4. CONCLUDING REMARKS

We have obtained two complementary formulations with regularized equations on compact state spaces for polytropic equations of state. This has allowed us to obtain a global picture of the solution space of these models. The two approaches revealed that certain solutions play an important role for the remaining solution structure.

The first approach (the  $\{\Sigma, K, y\}$ -formulation) showed that the regular scale-invariant solution, the self-similar Tolman solution, and a special non-regular solution (corresponding to the Tolman orbit) to a large extent determine the high energy density behavior of the regular solutions. Note that the non-regular Tolman solution is scale-invariant towards the origin. An approximate expressions for the metric coefficients for this solution has been given by deFelice *et al* [4].

The second approach (the  $\{U, V, y\}$ -formulation) revealed that when  $n > 3$  there exists another special solution (the one ending at  $P_4$ ) of great importance for the remaining solution structure. When  $3 < n < 5$  other solutions spiral around this “skeleton” solution. When  $n > 5$ , the regular solutions approach this solution and end at its endpoint  $P_4$ . This point is associated with a non-regular Newtonian solution, which describes the behavior of the regular solutions close to the surface when  $n > 5$ .

The dynamical behavior is particularly complicated when  $3 < n < 5$ . It is interesting to compare with Theorem 4 p 994 in Rendall & Schmidt [14], which in the present context states that regular relativistic polytropic models with  $1 < n < 5$  have finite radii if  $y_c$  is sufficiently small, and Theorem 1 p 60 in Makino [10], which in the present context states that when  $1 < n < 3$ , the radius of a regular model is finite. Makino also comments that the restriction of Rendall & Schmidt may be inevitable when  $3 \leq n < 5$  (p 62 in Makino [10]). For polytropes we have numerically shown

that *all* regular models are finite when  $n \lesssim 3.339$ . Thus, in this polytropic index range the restriction is *not* necessary. However, our investigation shows that for larger values of  $n$  it is. Our work shows that what is actually happening when  $3 < n < 5$  is determined in the relativistic regime and not the Newtonian regime, although this latter regime determines a finite number of possibilities. Considering the complicated dynamical behavior, it is hard to see how one could obtain our results except by numerics. Perhaps one could gain further insights by going beyond the static and spherical assumptions. For example, the behavior might be partly related to the stability features of the models.

We have shown that the present methods can be generalized to other equations of state. The state spaces in such cases are also 3-dimensional and this will make it possible to visualize the entire solution space for such equations of state as well. The first  $\{\Sigma, K, y\}$ -formulation should be useful when an equation of state behaves linearly or polytropically when the energy density goes to infinity. For such equations of state one could expect that the regular scale-invariant solution, the self-similar Tolman solution, and a special non-regular solution (the Tolman orbit), determine, to a large extent, the high energy density behavior of the regular solutions. The second  $\{U, V, y\}$ -formulation should be useful for equations of state that behaves polytropically when the energy density goes to zero. For such cases the low energy density regime should be described by the Newtonian boundary. An interesting question is what happens with the radius of a regular model when one has an equation of state that approaches a polytrope with index  $3 < n < 5$  asymptotically when  $p, \rho \rightarrow 0$ . It is probably determined in the relativistic regime, which depends on the actual equation of state. The relativistic polytropic equation of state nicely illustrates the above discussion. Since this equation of state is of considerable physical interest, we will treat this case in more detail in a future paper.

We think that the present type of approach nicely complements those used by Rendall & Schmidt [14] and Makino [10] and that they together should constitute useful tools for further explorations of relativistic star models.

## APPENDIX A

In this Appendix we will show how the different sets of variables can be derived. Starting with the line element in the form

$$ds^2 = -e^{2\phi} dt^2 + d\ell^2 + e^{2\psi-2\phi} d\Omega^2, \quad (\text{A.1})$$

and introducing variables according to

$$\theta = \dot{\psi}, \quad \sigma = \dot{\theta}, \quad B = e^{\phi - \psi}, \quad (\text{A.2})$$

where a dot denotes differentiation with respect to  $\ell$ , leads to the following expressions for the gravitational field equations

$$\dot{\theta} = -2\theta^2 + \theta\sigma + B^2 + 16\pi p, \quad (\text{A.3a})$$

$$\dot{\sigma} = -2\theta\sigma + \sigma^2 + 4\pi(\rho + 3p), \quad (\text{A.3b})$$

$$\dot{B} = (-\theta + \sigma)B, \quad (\text{A.3c})$$

$$8\pi p = \theta^2 - \sigma^2 - B^2. \quad (\text{A.3d})$$

This system looks very much like systems in spatially homogeneous cosmology (see, for example, Wainwright & Ellis [17]), even though the physical interpretation is quite different. Hence one can import ideas from treatments of spatially homogeneous models to the present situation.

To obtain the  $\{\Sigma, K, y\}$ -formulation, we use similar variables to the so-called expansion-normalized variables used frequently in spatially homogeneous cosmology (see Wainwright & Ellis [17]), and a dimensionless matter variable  $y$  according to

$$\Sigma = \frac{\sigma}{\theta}, \quad K = \frac{B^2}{\theta^2}, \quad y = \frac{p}{p + \rho}, \quad P = \frac{8\pi p}{\theta^2}. \quad (\text{A.4})$$

The new independent variable is determined by

$$\frac{d\ell}{d\lambda} = \frac{y}{\theta}. \quad (\text{A.5})$$

To obtain the  $\{U, V, y\}$ -formulation 2, we start with the Tolman-Oppenheimer-Volkoff approach

$$\frac{dp}{dr} = -\frac{(p + \rho)(m + 4\pi r^3 p)}{r(r - 2m)}, \quad (\text{A.6a})$$

$$\frac{dm}{dr} = 4\pi r^2 \rho, \quad (\text{A.6b})$$

(see, for example, [12]). We then introduce the variables  $\{U, V, y\}$  in terms of  $r, m, p$ , and  $\rho$ , according to the definitions (27) and (11), and a new independent variable defined by

$$\frac{dr}{rd\lambda} = (1 - y)(1 - U)F, \quad F = (1 - V)(1 - y) - 2yV. \quad (\text{A.7})$$

The relationship between the variables  $\{U, V\}$  and  $\{\Sigma, K\}$  is given by

$$U = \frac{(1 - \Sigma^2 - K)(1 - y)}{(1 - \Sigma^2 - K)(1 - y) + Ky - (1 - \Sigma)^2 y}, \quad (\text{A.8a})$$

$$V = \frac{(K - (1 - \Sigma)^2)(1 - y)}{K - (1 - \Sigma)^2 + 2y}. \quad (\text{A.8b})$$

### A.1. LANE-EMDEN VARIABLES

In the Lane-Emden approach, dimensionless variables variables  $\theta_{\text{LE}}, v_{\text{LE}},$  and  $\xi_{\text{LE}}$  are introduced according to

$$\theta_{\text{LE}} = \left(\frac{\rho}{\rho_c}\right)^{1/n}, \quad v_{\text{LE}} = \frac{A^3 m(r)}{4\pi\rho_c}, \quad \xi_{\text{LE}} = Ar, \quad (\text{A.9})$$

where  $A$  is a constant defined by

$$A = \sqrt{\frac{4\pi(1 - y_c)\rho_c}{(1 + n)y_c}}, \quad (\text{A.10})$$

(see, for example, Tooper [16]).

The relationship to the variables  $\{\Sigma, K, y\}$  is given by

$$\theta_{\text{LE}} = \frac{y(1 - y_c)}{y_c(1 - y)}, \quad (\text{A.11a})$$

$$v_{\text{LE}} = \left[ \frac{1 - \Sigma^2 - K}{8(1 + n)^3} \left(\frac{1 - y_c}{y_c}\right)^{3-n} \left(\frac{1 - y}{y}\right)^{1+n} \right]^{1/2} W, \quad (\text{A.11b})$$

$$\xi_{\text{LE}} = \left[ \frac{1 - \Sigma^2 - K}{2K(1 + n)} \left(\frac{y_c}{1 - y_c}\right)^{n-1} \left(\frac{1 - y}{y}\right)^{1+n} \right]^{1/2}, \quad (\text{A.11c})$$

where

$$W = \frac{K - (1 - \Sigma)^2}{K^{3/2}}. \quad (\text{A.12})$$

The relationship to the variables  $\{U, V, y\}$  is given by

$$\theta_{\text{LE}} = \frac{y(1-y_c)}{y_c(1-y)}, \quad (\text{A.13a})$$

$$v_{\text{LE}} = \left[ \frac{UV^3}{(1+n)^3(1-U)(1-V)^3} \left( \frac{y(1-y_c)}{y_c(1-y)} \right)^{3-n} \right]^{1/2}, \quad (\text{A.13b})$$

$$\xi_{\text{LE}} = \left[ \frac{UV}{(1+n)(1-U)(1-V)} \left( \frac{y_c(1-y)}{y(1-y_c)} \right)^{n-1} \right]^{1/2}. \quad (\text{A.13c})$$

### ACKNOWLEDGMENT

The authors wish to thank Alan Rendall and Bernd Schmidt for comments and for bringing important earlier work in the field to our attention. This research was supported by Gälöstiftelsen (USN), Svenska Institutet (USN), Stiftelsen Blanceflor (USN), the University of Waterloo (USN), and the Swedish Natural Research Council (CU).

## REFERENCES

1. H. Buchdahl, *Phys. Rev.* **116** (1959), 1027.
2. J. Carr, “Applications of center manifold theory”, Springer Verlag, New York, 1981.
3. S. Chandrasekhar, “An introduction to the study of stellar structure”, University of Chicago Press, Chicago, 1939.
4. F. deFelice, Y. Yu, and J. Fang, *Class. Quant. Grav.* **12** (1995), 739.
5. J. M. Goliath, U. S. Nilsson, and C. Uggla, *Class. Quant. Grav.* **15** (1998), 167.
6. J. M. Goliath, U. S. Nilsson, and C. Uggla, *Class. Quant. Grav.* **15** (1998), 2841.
7. J. B. Hartle, *Phys. Rep.* **46** (1978), 201.
8. G. P. Horedt, *Astron. Astrophys.* (1987) 177, 117.
9. H. Kimura, *Publ. Astron. Soc. Japan* **33** (1981), 273.
10. T. Makino, *Journal of Mathematics of Kyoto University* **38** (1998), 55.
11. C. W. Misner and D. H. Sharp, *Phys. Rev.* **136** (1964), B571.
12. C. W. Misner, K. S. Thorne, and J. A. Wheeler, “Gravitation”, Freeman and Co., New York, 1973.
13. U. S. Nilsson and C. Uggla, “General relativistic stars: Linear equations of state”, preprint 2000.
14. A. D. Rendall and B. G. Schmidt, *Class. Quant. Grav.* **8** (1991), 985.
15. K. Schwarzschild, *Sitzber. Deut. Akad. Wiss. Berlin, Kl. Math.-Phys. Tech.*, page 189, 1916.
16. R. F. Tooper, *Astrophys. J.* **140** (1964), 434.
17. J. Wainwright and G. F. R. Ellis, “Dynamical systems in cosmology”, Cambridge University Press, Cambridge, 1997.